Latin American Journal of
Solids and Structures
www.lajss.org

Finite element nonlinear analysis of high-rise unreinforced masonry building

A.H. Akhaveissy*

* Department of Civil Engineering, Faculty Engineering, Razi University, P.O. Box: 67149-67346, Kermanshah, Iran
Tel.:+98 831 427 4535; fax:+98 831 428 3264

Received 07 Oct 2011;
In revised form 10 May 2012

* Author email: Ahakhaveissy@razi.ac.ir

Abstract

A simple efficient algorithm based on compressive diagonal strength of unreinforced masonry walls is presented to determine capacity curve of unreinforced masonry building. The compressive strength is calculated based on a new close form solution. The new close form solution is determined based on predicted results using interface elements for modeling of mortar joints. Finite element method with two-noded linear elements is used for analyses. Different masonry structures, including low- and high-rise unreinforced masonry buildings, are analyzed using the new closed-form solution and the presented algorithm. A comparison of results of the present work with experimental data and other methods similar to the discrete element method show proper accuracy of the analyses in the present work. Consequently, the closed form solution with proposed algorithm can be used to satisfactorily analyze unreinforced masonry structures to predict the ultimate base shear force and the pushover curve. Hence, practicing engineers can determine the behavior of an URM building and its performance level with proper accuracy under seismic excitation using concepts described in the present work.

Keywords

Masonry wall, interface element, micro-modeling, macro-modeling, old masonry building, high-rise URM building.

1 INTRODUCTION

Masonry is the oldest building material that still finds wide use in today's building industries. Important new developments in masonry materials and applications have occurred in the past two decades. Masonry is a composite material that consists of units and mortar joints. Masonry buildings are constructed in many parts of the world where earthquakes occur. Hence, knowledge of their seismic behavior is necessary to evaluate the seismic performance of these types of building. Pushover analysis is commonly used to evaluate seismic performance and to determine the capacity curve. Therefore, the capacity curve is studied in this paper.

An approach for analysis of unreinforced masonry buildings is the macro-modeling of masonry as a composite material. The macro modeling is more practice oriented due to the reduce time and memory requirements as well as a user-friendly mesh generation. The compressive strength of a masonry unit is an important parameter in the analysis of unreinforced masonry buildings using the macro-element method. A masonry unit includes mortar joints and masonry bricks. The compressive strength for masonry units with different mortar was evaluated [10, 15, 16, 37, 38].

SAP2000 v.10, a software package with a user-friendly interface that is widely used by practicing engineers, was used for the seismic analyses of masonry buildings [31]. Two unreinforced stone masonry walls in the Catania Project were modeled with SAP2000 v.10. The static pushover curves from the analyses were compared with predicted results from the SAM code, which was developed by the University of Pavia, the Genoa research group and the Basilicata research group [31]. The Basilicata research group used a no-tensile-strength macro-element model with crushing and shear failures while the Genoa research group used a finite element model with layer failures. The ultimate base shear force for wall A is predicted to be 1682 kN by the Genoa R.G., 1339 kN by SAP2000, 1115 kN by the SAM code, and 1395 kN by the Basilicata R.G. Accordingly, the ultimate base shear force for wall B is predicted to be 650 kN by the Genoa R.G., 474 kN by the SAM code and SAP 2000, and 508 kN by the Basilicata research group. These results show differences between the different studies. Hence, practicing engineers may be confused as to which codes or research is the most applicable or precise.

The in-plane shear behavior of hollow brick masonry panels was evaluated [14]. The nonlinear behavior of masonry was modeled assuming elastic-perfectly plastic behavior, Drucker-Prager, of the mortar joint in the ANSYS 5.4 commercial software. In other words, the micro-element method was used to analyze the panels. A comparison between the experimental results and numerical analysis shows good agreement.

A macro-element approach to the three-dimensional seismic analysis of masonry buildings was applied [5]. The full model displays a base shear force that is approximately 25% higher than the value calculated for the plane structure.

Seismic fragility of an unreinforced masonry low-rise building was studied using a structural modeling method. The method utilizes a simple, composite nonlinear spring. In this method, the wall is divided into distinct areas or segments. Each segment of the unreinforced masonry wall is then represented by a nonlinear spring, and the springs are assembled in series and in parallel to match the segment topology of the wall [30]. Rota et al.[33] presented a new analytical approach for the derivation of fragility curves for masonry buildings. The methodology was based on nonlinear stochastic analyses of building prototypes. Monte Carlo simulations were used to generate input variables from the probability density functions of mechanical parameters.

The seismic performance of existing unreinforced masonry buildings in North America were considered in a state-of-the-art paper [7]. The various failure modes of unreinforced masonry buildings subjected to earthquake excitation were described in the paper. The damage to the existing buildings for different earthquake scenarios was evaluated.

The static pushover curve was studied using the boundary element method for unreinforced masonry walls [3]. In the analysis, a no-tension-material with an infinite strength in compression was adopted to model the masonry buildings. The predicted results show good agreement with experimental data.

Milani et al. [24] performed a three-dimensional homogenized limit analysis to determine the ultimate lateral load of full masonry structures. Linearized homogenized surfaces for masonry in six dimensions [9, 23] were obtained and implemented in a finite element code. Comparisons between the predicted results from the 3D homogenized limit analysis and experimental data show an error of approximately 12%. Milani et al. [26] also used a 3D homogenized limit analysis for full masonry buildings reinforced by FRP. The error between the predicted results and experimental data for a two-story masonry building is 4.6% in absence of FRP and 9.4% in presence of FRP. Milani [20, 21] applied the 3D homogenized limit analysis to determine the limit load of a wall under in-plane and out-plane loading.

A simple equilibrium model was used to estimate the ultimate capacity of masonry shear walls. The model was based on strut-and-tie schemes representing the combination of the compression or tension stress fields at the ultimate condition. Comparisons between the performance of the model and experimental results for dry-joint and mortar-joint masonry show good agreement. [32]

A finite element analysis was conducted for a single-story, one-room masonry building, with different aspect ratios and with different positions of wall openings, subjected to a seismic force with varying direction [36]. The response spectrum method was employed for the analysis. The predicted results show that the critical direction of seismic force for the development of maximum stresses in the walls of a room occurs when the opening is along the short wall of the room. It was also observed that the maximum principle tensile stress occurred in the short wall, and the maximum shear stress occurred in the long wall.

The analysis of unreinforced masonry buildings employed a two-step approach [22]. In step 1, the ultimate bending moment – shear force strength domains of the masonry spandrels were derived by means of a heterogeneous upper-bound finite element limit analysis, and the results were stored in a database. In step 2, an equivalent frame model of the masonry wall was assembled. In the frame model, the spandrels were modeled as elastic Timoshenko beams. At each analysis step, a check was performed to determine whether the internal forces of these coupling beams were smaller than the failure loads stored in the database created in step 1. The shear force and bending moment capacity of the piers were simply estimated according to the Italian Design code. The proposed analysis approach was appeared capable of deriving the pushover curve of unreinforced masonry walls [22].

A constitutive model was developed on the basis of homogenized anisotropic elasto-plasticity. The effect of anisotropy was introduced by a fictitious isotropic stress and strain space. The advantage of this model is that the classical theory of plasticity can be used to model nonlinear behavior in the isotropic spaces [17].

A rigid-body numerical model was used to identify the minimum height-to-thickness ratio that would cause the wall to collapse when subjected to different out-of-plane ground motions

[35]. The spectral accelerations of the ground motions were selected to be 0.24 g, 0.3 g, 0.37 g and 0.44 g. The model was calibrated using the results of full-scale shake table tests of a wall with a height to thickness ratio of 12 [19]. The results of the analysis showed that when a wall is subjected to a spectral acceleration of 0.44 g, the probability of collapse for height-to-thickness ratios less than 10 is less than 1%. The ratios for spectral accelerations of 0.24 g and 0.3 g are 18 and 15, respectively [35]. Therefore, walls with the conditions described above will stabilize when subjected to out-of-plane ground motions, and the in-plane strength of the wall will be important in resisting lateral forces.

Akhaveissy [1] presented a new close form solution to determine the shear strength of unreinforced masonry walls. Predicted results show less error percentage than ATC and FEMA-307 [12]. The new explicit formula is based on results of proposed interface model by Akhaveissy [1]. Consequently, the proposed closed form solution can be used satisfactorily to analyze unreinforced masonry structures.

The research results discussed above that are related to macro-modeling processes show considerable differences between different methods of macro-modeling in comparison with test data [31]. Therefore, in this investigation, the closed-form solution by Akhaveissy [1] is extended to allow implementation in a macro-element approach using two-noded linear elements in a finite element framework. The analysis time is decreased in comparison with analyses performed using the micro-element approach and the finite element method, which use solid elements and shell elements. Moreover, the accuracy of the analysis is increased because the formulation is based on the micro-element approach.

2 THE CLOSE FORM SOLUTION

The closed form solution to determine the resistance lateral force of unreinforced masonry wall is based on the effective width of the wall in compression [1]. The effective width of unreinforced masonry wall is in terms of the height-to-width ratio of the wall. The width of the compressive diagonal is proposed as a coefficient of the length of the diagonal [1]. This coefficient is shown by F_w. Fig. 1 shows variations of the coefficient versus different height/width ratio of the wall [1].

Hence, the resistance lateral force is based on compressive axial force of the effective width, Fig. 2.

According to Fig. 2, the resistance lateral force is as follows [1]:

$$\begin{aligned} &P = P_d * COS(\theta) \\ &P_d = F_w L_d t \sigma_d \ ; \ \sigma_d = 2\,\tau_u \\ &\tau_u = C + \sigma_0 \tan(\phi) \end{aligned} \tag{1}$$

where, C and ϕ are the cohesive strength and the friction angle, respectively. In Eq. (1), σ_0 is the initial applied pressure on the top of the wall. The lateral strength of different unreinforced masonry walls analyzed by Eq. (1) and Fig. 1 [1]. Predicted results compared with test data and FEMA guideline [12]. The comparisons show good correlation between predicted results

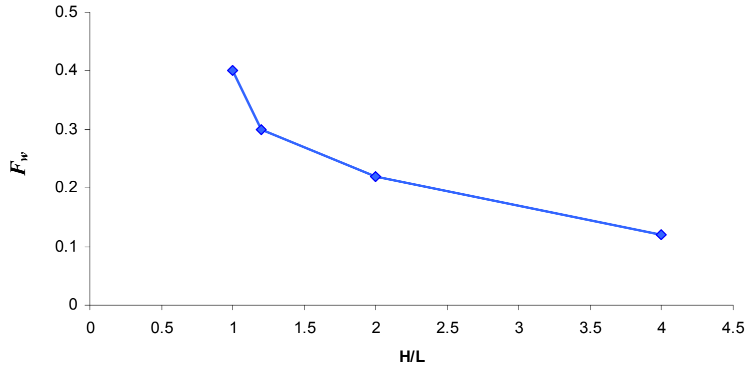

Figure 1 The coefficient of compressive diagonal versus high to width ratio of wall [1]

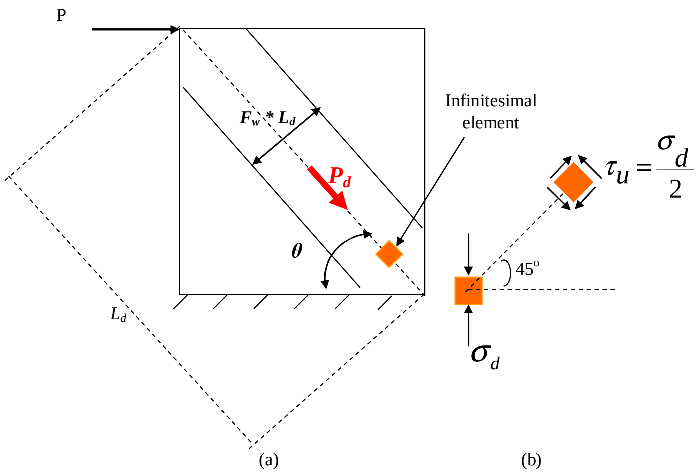

Figure 2 a) compressive effective width of the wall and b) principal stress on infinitesimal element [1]

of Eq. (1) and test data. The closed form solution, Eq. (1), predicts the ultimate lateral load of unreinforced masonry walls less error percentage than ATC and FEMA-307 [12]. Hence, Eq. (1) is used to determine the shear strength of piers and spandrels in an unreinforced masonry frame. Therefore, the internal forces of two-noded linear elements in finite element method are compared with predicted strength by Eq. (1).

3 MACRO-ELEMENT MODEL

In this study, different unreinforced masonry (URM) structures are analyzed based on Eq. (1). A macro-element method is used for the analysis of URM structures based on two-noded linear elements. Then, a force–displacement relationship and an algorithm are presented to analyze URM structures using macro-elements. The stiffness matrix of the element included both bending and axial stiffness matrices. Fig. 3 shows the shape functions of the elements for both parts.

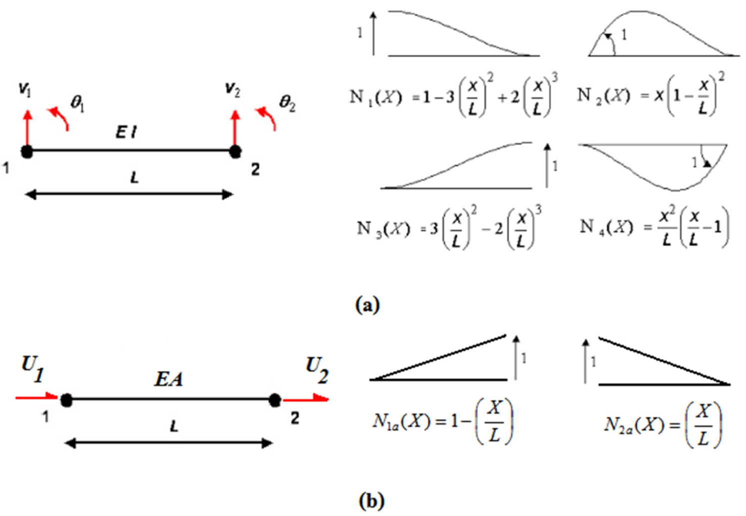

Figure 3 Bernoulli beam element and shape function for the a) bending effect and b) axial effect

The initial stiffness method is used in the analysis. Therefore, assuming a linear elastic material with a stress-strain relationship of $\{\sigma\} = [E]\{\varepsilon\}$ and a strain-displacement relationship of $\{\varepsilon\} = [B]\{d\}$, the element bending stiffness matrix can be determined from the following relationship:

$$K_b = \int_0^L [B]^T [EI][B]\,dx\,;\quad [B] = \frac{d^2}{dx^2}\begin{bmatrix} N_1 & N_2 & N_3 & N_4 \end{bmatrix} \tag{2}$$

After integration using the element shape functions, the elemental bending stiffness K_b is found to be the following:

$$K_b = \frac{EI}{L^3}\begin{bmatrix} 12 & 6L & -12 & 6L \\ 6L & 4L^2 & -6L & 2L^2 \\ -12 & -6L & 12 & -6L \\ 6L & 2L^2 & -6L & 4L^2 \end{bmatrix} = \begin{bmatrix} K_{b11} & K_{b12} \\ K_{b21} & K_{b22} \end{bmatrix} \tag{3}$$

The element axial stiffness matrix can be expressed using the following relationship:

$$K_a = \int_0^L [B]^T [EA][B]\,dx\,;\quad [B] = \frac{d}{dx}\begin{bmatrix} N_{1a} & N_{2a} \end{bmatrix} \tag{4}$$

After integration using the element shape functions, the elemental axial stiffness K_a is found to be the following:

$$K_a = \frac{EA}{L}\begin{bmatrix} 1 & -1 \\ -1 & 1 \end{bmatrix} = \begin{bmatrix} K_{a11} & K_{a12} \\ K_{a21} & K_{a22} \end{bmatrix} \tag{5}$$

The elemental stiffness for the local axis is obtained by combining Eq. (3) and Eq. (5) to arrive at the following equation:

$$K = \begin{bmatrix} K_{a11} & 0 & K_{a12} & 0 \\ 0 & K_{b11} & 0 & K_{b12} \\ K_{a21} & 0 & K_{a22} & 0 \\ 0 & K_{b21} & 0 & K_{b22} \end{bmatrix} \tag{6}$$

The stiffness matrix of elements in the global axis is determined using rotation forces from the local axis to the global axis and is expressed as the following:

$$K_G = [R]^T [K] [R]$$

$$[R] = \begin{bmatrix} R_1 & 0 \\ 0 & R_2 \end{bmatrix} \; ; \quad R_1 = R_2 = \begin{bmatrix} \cos\theta & \sin\theta & 0 \\ -\sin\theta & \cos\theta & 0 \\ 0 & 0 & 1 \end{bmatrix} \tag{7}$$

Here, $\theta$is the angle between the axis of the element and the horizontal axis in the anticlockwise direction.

The solution to the equilibrium equation system yields the joint displacements and internal forces in the local coordinate system. The internal forces cause damage to the masonry wall. Therefore, the internal forces should be compared with the nonlinear behavior of masonry walls. This comparison is discussed in the next section.

3.1 Deformation capacity and stiffness evaluation

The response of brick masonry walls is strongly nonlinear, even at low load levels, because of the low tensile strength of the bed and head joints. As the damage due to cracking increases, masonry walls show both strength and stiffness degradation. A definition of the elastic stiffness of a wall subjected to in-plane shear must be related to a reference stress or deformation. A common approach followed for design and assessment purposes is to idealize the cyclic envelope with a bilinear curve. In Fig. 4, possible definitions of the parameters of the bilinear curve are presented. The value of V_u is determined by Eq. (1). In other words, $V_u$is equal to parameter P in Eq. (1). The initial elastic stiffness of a masonry wall is evaluated using Eq. (7). Fig. 4 also shows the acceptance criteria for the primary elements according to FEMA 356 [13]. Accordingly, the value of drift for the immediate occupancy criterion, the life safety level and the collapse prevention level are 0.1%, 0.3% and 0.4%, respectively. The acceptance criteria provided by FEMA356 [13] are also valid when evaluating damage to unreinforced masonry structures. However, the ultimate shear force for piers and spandrels is determined by Eq. (1).

3.2 Proposed algorithm

An algorithm is proposed for nonlinear analysis of URM structures based on the macro-element method and a force–displacement relationship. Table 1 shows the solution process.

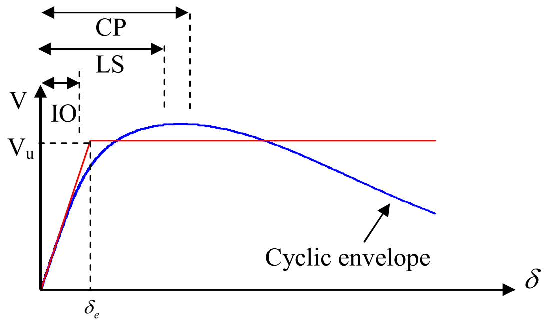

Figure 4 Definition of an equivalent bilinear envelope

Table 1 Proposed algorithm

1	definition of geometry, material and loading, including the dead and live load and lateral load
2	determination of the elastic stiffness matrix for each element based on Eq. (7) and the stiffness matrix of the total structure
3	determination of the dead and live load vectors for the URM structure
4	solution of the system of equations for step 3
5	establishment of the incremental load vector for the lateral load
6	solution of the system of equations based on step 2
7	determination of the internal force vector in the local axes for each element
8	evaluation of the internal forces for nonlinear behavior (see Table 2)
9	determination of the residual force vector for the URM structure
10	evaluation of the convergence criterion based on the L2 norm of the residual force
11	if the value of the L2 norm is less than the value of the error provided by the user, then go to step 5 and evaluate the last incremental lateral force vector, otherwise go to step 6 and solve the system of equations for the residual force vector

A program in the FORTRAN language is prepared from the algorithm presented in Tables 1 and 2. Different unreinforced masonry structures are analyzed using the program. Predictions from the program are compared with laboratory data and numerical analyses based on different solution procedures.

4 APPLICATIONS

4.1 A single-story unreinforced masonry building

A full-scale single-story unreinforced masonry building tested in the laboratory by Paquette and Bruneau [27–29] was chosen to validate the model. Fig. 5 shows the west wall of the tested model. The parapet of the west wall and the east wall was 254 mm tall[27].

The compressive strengths of the brick and mortar were 109 and 9.24 MPa, respectively, and the compressive and tensile strengths of the masonry were 22.2 and 0.18 MPa, respectively [27]. These strengths were used for the numerical analysis of the west wall by the DSC/HISS-CT model [2]. The thickness of the wall was 190 mm. The gravity load, 2.4 kN/m ^{2}, was applied on the diaphragm, whose dimensions were 4091 mm * 5610 mm. Ten wood joists were

Table 2 Evaluation of URM wall resistance

1	Determine F_w using Fig. 1. F_w for H/L greater than 4 is determined from a linear equation between H/L=2 and H/L=4 However, if $F_w \leq 0 \Rightarrow F_w = 0$
2	determination of the axial stress, σ, based on the axial force, P, in the local axes. The axial stress is assumed negative for tensile stress and positive for compressive stress.
3	if $\sigma \leq$ then
	$if\, \sigma < -f_t\ then$
	$Value\, of\, all\, internal\, forces\, is\, assumed\, equal\, to\, zero$
	$else$
	$\tau_u = C + \sigma\ \tan(\varphi)$
	$if\, \tau_u\ < 0\, then\ \tau_u\ =\ 0$
	$\sigma_d = 2 * \tau_u$
	$V_u\ =\ F_w L_d t \sigma_d$
	$if\ V_u\ >\ V_{int}\, then\, the\, behavior\, of\, the\, wall\, is\, elastic\, and\, internal\, shear$
	$force,\ V_{int},\ is\, not\, changed$
	$if\ V_u\ \leq\ V_{int}\, then$
	$f = \frac{V_u}{V_{int}}$
	$V_{int}\ =\ V_u\ *\ \frac{V_{int}}{\lvert V_{int}\rvert}$
	$M_{int} = M_{int} * f$
	$endif$
	$endif$
	$else$
	$if\, \sigma >\ f_c\, then$
	$\sigma = f_c$
	$P = \sigma * A * \frac{P}{\lvert P\rvert}$
	$endif$
	$\tau_u = C + \sigma\ \tan(\varphi)$
	$\sigma_d = 2 * \tau_u$
	$V_u\ =\ F_w L_d t \sigma_d$
	$if\ V_u\ >\ V_{int}\, then\, the\, behavior\, of\, the\, wall\, is\, elastic\, and\, internal\, shear$
	$force,\ V_{int},\ is\, not\, changed$
	$if\ V_u\ \leq\ V_{int}\, then$
	$f = \frac{V_u}{V_{int}}$
	$V_{int}\ =\ V_u\ *\ \frac{V_{int}}{\lvert V_{int}\rvert}$
	$M_{int} = M_{int} * f$
	$endif$
$end,\ if$	

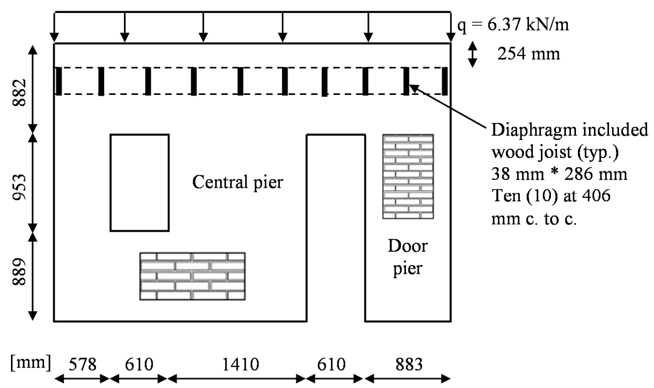

Figure 5 Dimensions of the west wall in mm [27]

applied to the diaphragm to transmit the gravity load to the west and east walls. The net span of the wood joist was 5310 mm [27]. Therefore, the gravity load on each wall was 6.37 kN/m. The mesh for the west wall contained 720 eight-node isoparametric elements and 2527 nodes; the number of degrees of freedom was 4926 [2]. The west wall was also analyzed to determine the ultimate base shear force by Akhaveissy [1]. The cohesion strength and the friction angle for the analysis were equal to 0.078 MPa and 31.9 degree, respectively [1]. The wall is chosen to show capability of the proposed algorithm in Table 1 and 2. Fig. 6 shows the equivalent frame model for the analysis. The number of degrees of freedom in present work is 9 and the error for the evaluation of convergences is considered to be 1e-10.

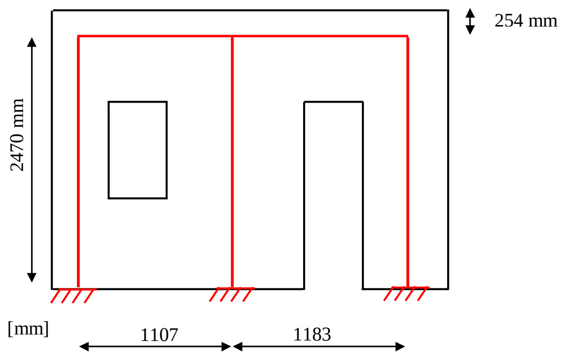

Figure 6 Equivalent frame model for the west wall

Test data and predicted results in present work are compared in Fig. 7. Predicted pushover curve shows good correlation with test data. Fig. 7(b) shows comparison of the results for displacement at top of wall between 0 to 3 mm. The predicted base shear force by DSC/HISS-CT model and Equivalent frame model are 22.7 kN and 22.5 kN, respectively. Value of the base shear force is observed 22.8 kN [27]. Hence, the ultimate lateral load is estimated with proper accuracy by both models.

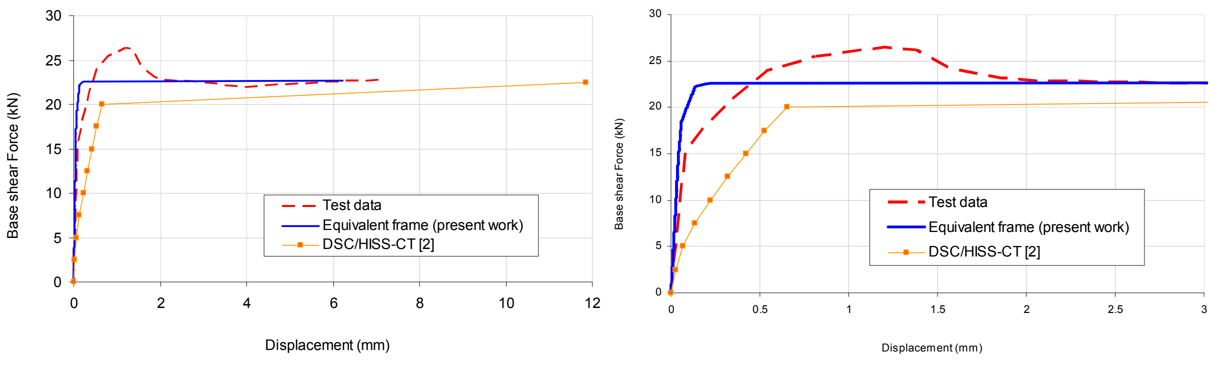

Figure 7 a) Comparison of predicted results with test data for the west wall and b) detailed illustration of the results

The initial slop of the equivalent frame in present work correlates with test data, Fig. 7(b). However, predicted results by DSC/HISS-CT [2] shows less accuracy than the equivalent frame.

4.2 A two-bay, two-story building

A full-scale, two-story unreinforced masonry building tested at Pavia University was chosen for model validation [18]. This structure has been extensively studied in the literature [4, 8]. The building, with a 6*4.4 m floor plan and 6.4 m in height, contains an almost independent shear wall that is in-plane loaded. The wall considered here (named the “door wall”) is 250 mm thick and has two doors on the first story and two windows on second story, as shown in Fig. 8. The door wall includes two exterior piers and one interior pier. The exterior pier width and axial loads on the bottom and top levels are equal to 1.15 m, 56 kN and 26.9 kN, respectively. The interior pier width and axial loads on the bottom and top levels are equal to 1.82 m, 133 kN and 64.5 kN, respectively.

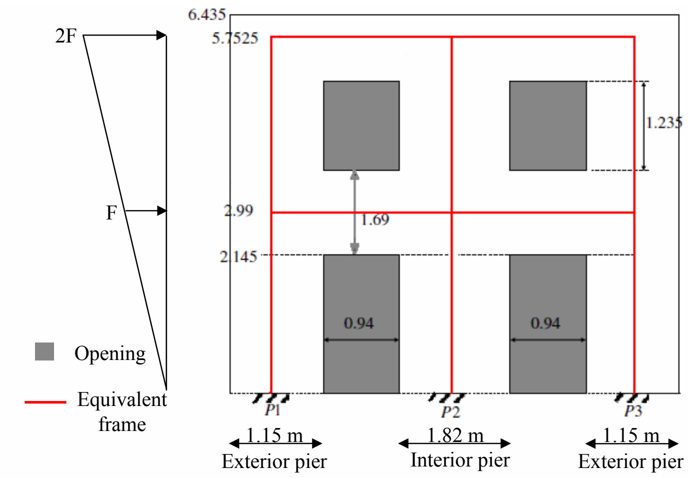

Figure 8 Door wall of the full-scale, two-story unreinforced masonry building tested at Pavia University

The properties of the structure used in the model are summarized below[4]:

The maximum compressive strength of a masonry prism, f_m, is equal to 7.9 MPa. The joint tensile strength and the joint cohesion are 0.07 MPa and 0.14 MPa, respectively. The joint coefficient of friction is 0.55. The shear modulus is equal to the effective value, $G_{eff} = 90f_m$. Fig. 9 shows comparisons between the present work and experimental data and numerical analyses [8]. Calderini et al. [8] used the finite element method (FEM) to analyze the two-story unreinforced masonry building tested at Pavia University. The model included 2696 nodes and 5128 triangular shell elements. The predicted results were compared with results obtained using the equivalent frame model and the Tremuri software [8]. The equivalent frame included 9 nodes, and 3 nodes were fully constrained at the base. The reduce stiffness and full stiffness were used to analyze the building with the equivalent frame.

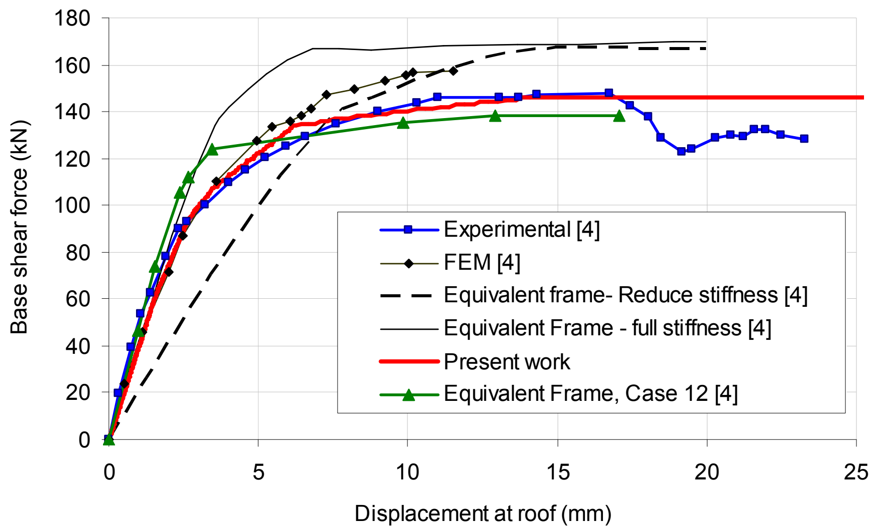

Figure 9 Comparison of the predicted results with experimental data for the two-story unreinforced masonry building tested at Pavia University

Fig. 9 shows that the equivalent frame–reduce stiffness model predicted that the stiffness of the building would be lower than the real stiffness. The value of the ultimate base shear force from the Tremuri software was estimated to be 167 kN whereas the experimental value was determined to be 147 kN. The value of ultimate base shear force from the present work and from Belmouden and Lestuzzi [4] was predicted to be 147 kN and 137.6 kN, respectively. The finite element method estimate of the force was 157 kN. Fig. 9 shows a better agreement between the test data and the present work than with other models. To consider the damage to the structure, the acceptance criteria are evaluated in Fig. 10. The equivalent frame in the present work included 9 nodes, and 3 nodes were fully constrained at the base. The applied base shear force equal to the lateral load is 150 kN, which is prepared in 400 steps. The tolerance for both the displacement convergence criterion and the force convergence criterion is $1{*}10^{-10}$. The analysis of the URM structure for step 389 converged after 1434 iterations whereas the analysis is not converged after 45,000 iterations for step 390. The total time of the calculation is 4.78 sec. The value of the displacement at the roof for step 389, after 1434 iterations, is 14.10 mm; however, the value of the displacement for step 390 after 45,000 iterations is 179.23 mm.

Crack patterns from the experimental test of the URM building at the failure state (a top displacement equal to 24 mm) show damage to the piers for the second story and the first story as well as damage to the spandrels at the first floor. The predicted failure of the piers correlates with the observed data while the damage to the spandrels is not seen in the present work. This difference is due to the dissipation of energy by the piers. Hence, the spandrel beams behave as elastic beams.

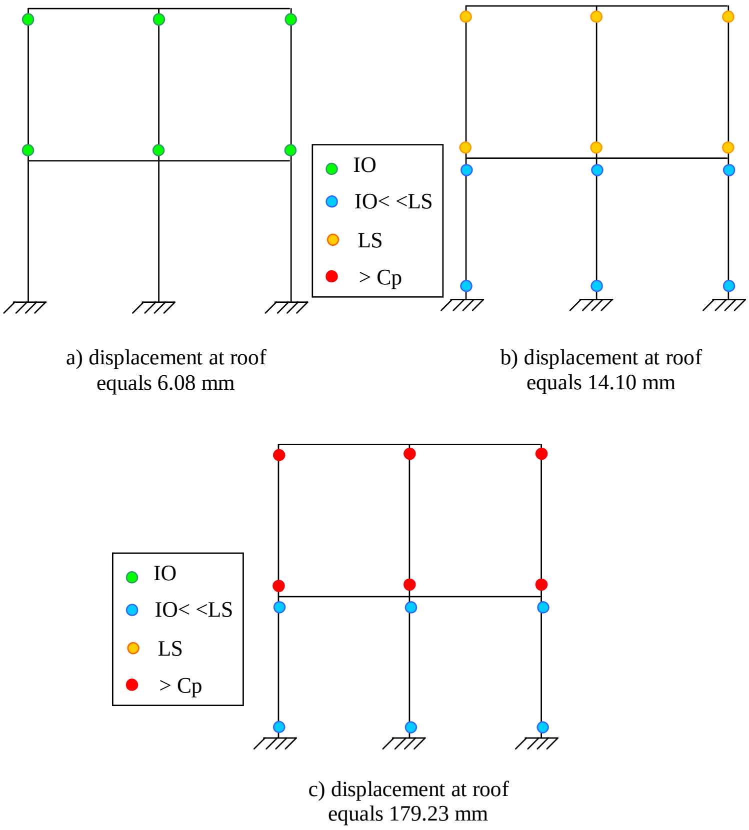

Figure 10 Damage levels for the URM structure from the present work for a) displacement at the roof equals 6.08 mm, b) displacement at the roof equals 14.10 mm and c) displacement at the roof equals 179.23 mm

4.3 A seven-bay, two-story building

In the present work, two different unreinforced masonry building are analyzed. A one-bay frame and a seven-bay frame with two stories are analyzed to evaluate the capability of the model. The structures are shown in Fig. 11. These unreinforced masonry frames were analyzed by Salonikios et al. [34]. Details of the structures are explained as follows. In addition to the self-weight of the masonry, extra masses are considered at the floor levels. For the one-bay frame, a uniformly distributed mass of 6 tons/m was assumed for the first floor, and 4 tons/m was assumed for the second floor [11, 34]. The corresponding values for the seven-bay frame were assumed to be 3 and 2 tons/m, respectively [34]. The mechanical characteristics of the masonry material were as follows: the thickness of the walls was equal to 0.6 m, the volumetric mass was $\rho = 2t/m^3$, the Young's modulus was E=1650 MPa, the Poisson ratio was $\nu = 0.2$, the tensile strength was f_t=*0.1* MPa, and the compressive strength was f_c=3.0 MPa. The joint cohesion and the joint friction angle were 0.09 MPa and 30 ^{o}, respectively [34].

Fig. 12. shows equivalent frames for the one-bay and seven-bay two-story masonry buildings with the lateral load pattern.

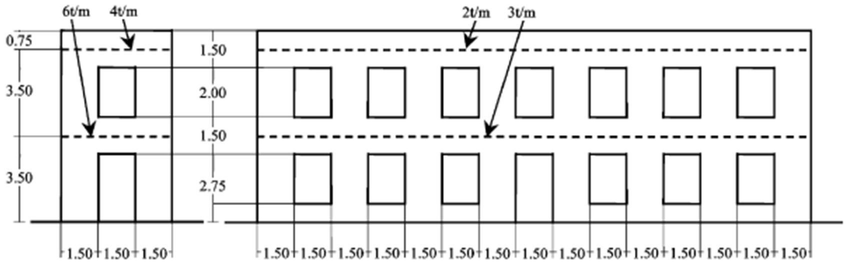

Figure 11 a) One-bay and b) seven-bay two-story masonry buildings

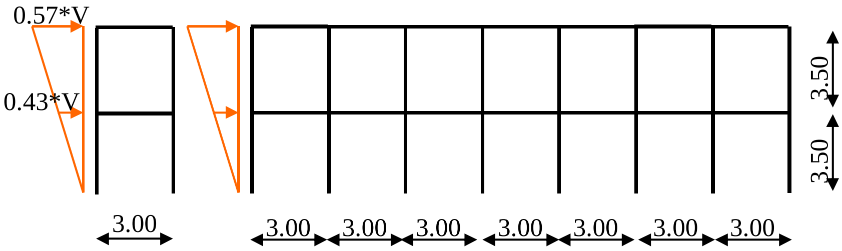

Figure 12 Equivalent frame and lateral load pattern for a) one-bay and b) seven-bay two-story masonry buildings

In Fig. 12, V is the value of the base shear force on the masonry buildings at the failure mode. Each node in Fig. 12 included two transitive degrees of freedom and one rotational degree of freedom. Hence, the numbers of degrees of freedom for the one-bay building and the seven-bay building are 12 and 48, respectively. The total number of elements for the masonry buildings in Fig. 12(a) and (b) are 6 and 30, respectively. Salonikios et al.[34] used the equivalent frame and discrete element methods to analyze the one-bay and seven-bay buildings. The presented relations in the FEMA guidelines were used in the equivalent frame method. The number of elements and degrees of freedom for both masonry buildings were the same as in the present work. The number of nodes, degrees of freedom and elements were 518, 1008 and 444, respectively, for the one-bay, two-story building in the discrete element method. Salonikios et al. [34] used element dimensions of 0.2*0.1 for the one-bay frame and 0.5*0.25 for the seven-bay frame. Hence, the number of nodes, degrees of freedom and elements were 2402, 4632 and 2100, respectively, for the seven-bay frame in the discrete element method. Consequently, the solution time is less with the equivalent frame method. The solution time in the present work using the equivalent frame model is 0.3 and 0.7 sec for the one-bay and seven-bay frames, respectively. The tolerance for both the displacement and the force convergence criteria is 1e-5 for the one-bay frame and 1e-12 for the seven-bay frame. The total number of converged steps is 49 steps out of 50 steps for the one-bay frame and 33 steps out of 50 steps for the seven-bay frame. The analysis of the one bay structure for step 49 converged after 161 iterations whereas the analysis is not converged after 400 iterations for step 50. The analysis of the seven bays structure for step 33 converged after 1396 iterations. A comparison of the pushover curve from the present work and that predicted by Salonikios et al. [34] is shown in Fig. 13 for both buildings. The value of the displacement at the roof of one bay frame for step 49, after 161 iterations, is 15.163 mm; however, the value of the displacement for step 50 after 400 iterations is 27.994 mm. The value of the displacement at the roof of seven bays frame for step 33 is 11.33 mm; however, the value of the displacement for step 34 after 1400 iterations is 141.699 mm.

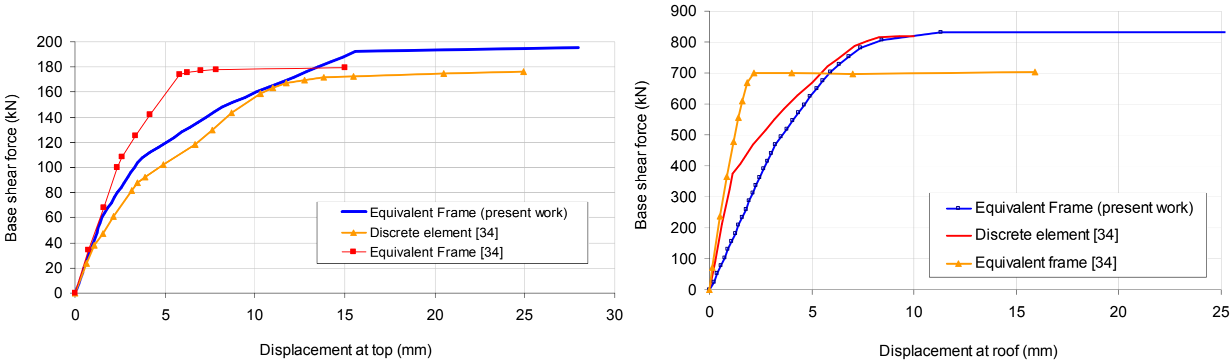

(a) the pushover curve for the one-bay, two-story masonry building

(b) the pushover curve for the seven-bay, two-story masonry building

Figure 13 Comparisons of the pushover curves from the equivalent frame model and the discrete element method

The values of the base shear force for the one-bay and seven-bay masonry structures predicted in the present work are 190 kN and 794 kN, respectively. These values are 177 kN and 819 kN when using the discrete element method and 180 kN and 705 kN using the equivalent frame method as presented in the study by Salonikios et al.[34] . Accordingly, the predicted results in present work correlate well with the results of the discrete element method. The predicted pushover curve from the equivalent frame model by Salonikios et al. [34] shows a nearly elastic-perfectly plastic behavior; however, the predicted pushover curve from the equivalent frame model in present work shows a flexible behavior that is similar to the curve from the discrete element method with the numerous number of degrees of freedom. Fig. 14 shows the plastic hinges for the masonry structures in accordance with points A and B in Fig. 13.

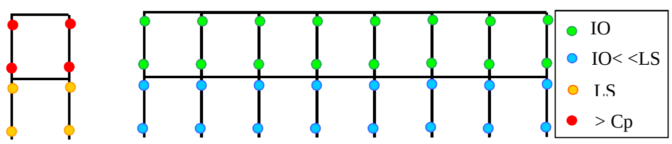

a) displacement at roof equals 27.994 mm

b) displacement at roof equals 11.33 mm

Figure 14 The plastic hinges for the one-bay and seven-bay two-story masonry buildings from the present analysis for points A and B in Fig. 13

4.4 Application to an old masonry building

An inner wall of a five-story building located in Via Martoglio (Catania, Italy) is analyzed using Eq. (1) and the presented algorithm, as shown in Tables 1 and 2. The full geometric characterization of the panel in the present analysis is shown in Fig. 15. The building was analyzed by Brencich et al. [6]. The four-node element with 2*2 Gauss points was used in the analysis. The model included 17,000 degrees of freedom. This building was also analyzed by Milani et al. [25]. The lower bound analysis utilized 1000 triangular elements. The thickness of last story is 160 mm while the thickness of the other stories is 300 mm. Numerical values used in the present analysis, as shown in Table 3, are adopted from Brencich et al.[6].

Table 3 Mechanical properties of the masonry unit and joints [6]

c (MPa)	f_t (MPa)	f_m (MPa)	ϕ
0.15	0.1	3.00	26.56

Here, f_t is the tensile strength, f_m is the compressive strength, c is the cohesion and ϕ is the friction angle.

The equivalent static forces at the levels of stories were calculated in Brencich et al.[6] , as shown in Table 4.

Table 4 Equivalent static forces for the five-story masonry building [6]

Unit weight of masonry $\gamma = 17\,kN/m^3$						
Level	0	1	2	3	4	5
Thickness of wall (mm)	300	300	300	300	300	160
Masonry weight (kN)	264.70	480.55	486.70	486.70	373.15	129.80
Applied load on stories (kN)	305.05	305.05	372.90	372.90	372.90	53.70
Total weight (kN)	569.75	785.60	859.60	859.60	746.05	183.50
h_i (m)	0.64	4.52	8.22	11.92	15.62	19.12
$\gamma_i = h_i \sum_{j=1}^{n} W_j / \sum_{j=1}^{n} W_j h_j$	0.0704	0.4974	0.9045	1.2786	1.7187	2.1038
$F_h = W * C * R * \varepsilon * \beta * I * \gamma$	$I = 1.$	$\varepsilon = 1.$	$R = 1.$	$\beta = \beta_1 * \beta_2 = 4.$	$S = 12 \Rightarrow$	$C = 0.1$
Equivalent static force F_h (kN):	16.05	156.30	311.00	439.65	512.90	154.40

The equivalent frame model and the seismic loads on the old five-story masonry building are shown in Fig. 16.

The equivalent frame model in present work included 75 linear elements and 120 degrees of freedom (DOFS). The tolerance for both the displacement convergence criterion and the force convergence criterion is $1*10^{-12}$. The model is analyzed using the algorithm in Tables 1 and 2. The total time of the calculation is 144 sec. The predicted pushover curve from the present analysis is compared in Fig. 17 with a predicted curve using the discrete element method with 17,000 DOFS.

Fig. 17 shows good agreement between the results of the equivalent frame model and the discrete element method for the hardening branch. The value of the ultimate base shear force is 1430 kN using the equivalent frame model and 1258 kN using the discrete element method.

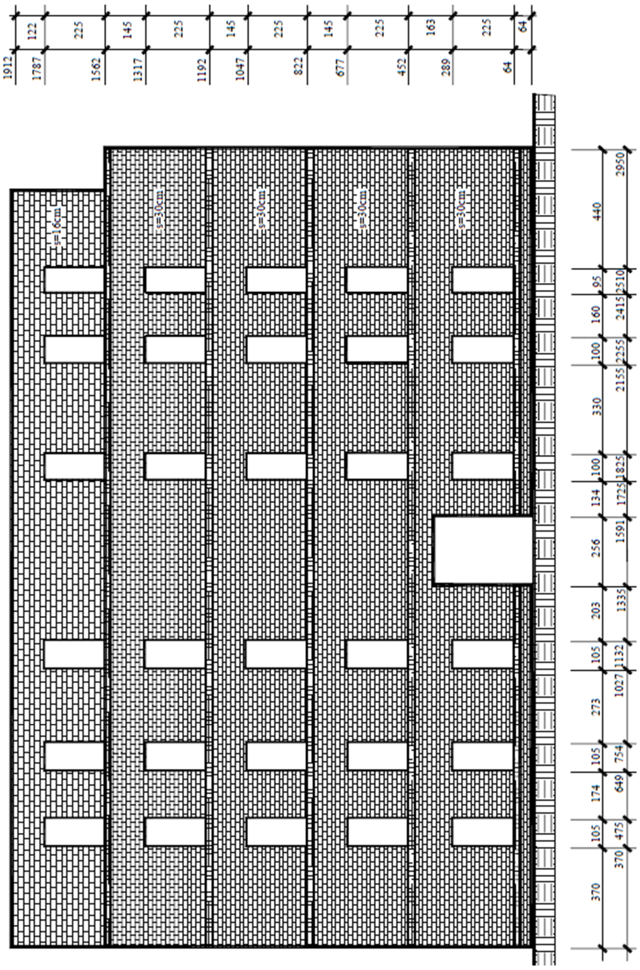

Figure 15 Geometric diagram of the inner wall of a five-story building [6]

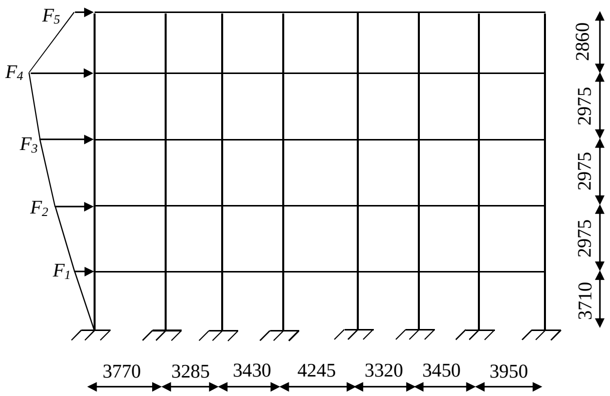

Figure 16 Equivalent frame model and seismic loads

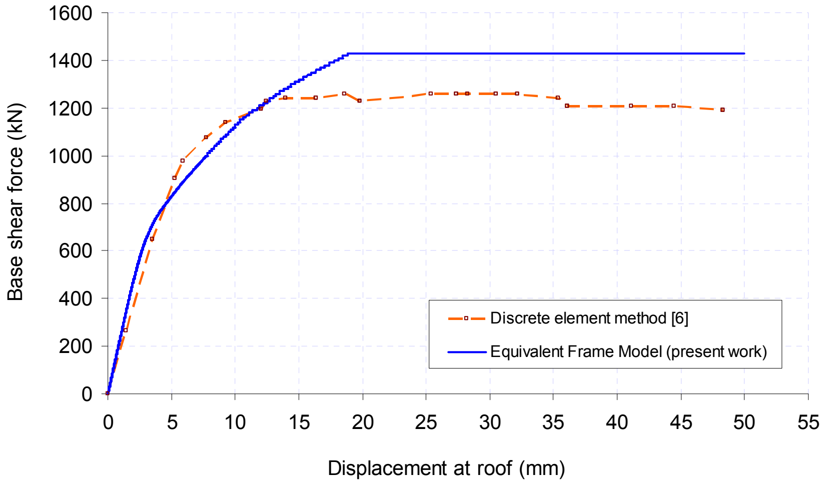

Figure 17 Comparison of the results from the present work with 120 DOFS and the discrete element method with 17,000 DOFS

The difference between the ultimate base shear forces for both models is less than 13.7%. Fig. 18 shows the distribution of the plastic hinges in accordance with point A in Fig. 17. When the displacement of the roof equals 49.963 mm, point A in Fig. 17, the performance level of the masonry piers in the first floor is between the immediate occupancy level and the life safety level, and the value of the drift for the piers is 0.002. The performance levels of the masonry piers for other stories indicate previous collapse, and the values of the drift for the piers are variable and between 0.0033 and 0.0037.

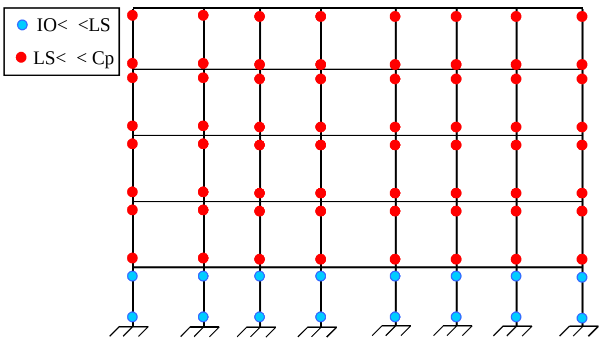

Figure 18 Distribution of plastic hinges for the old five-story unreinforced masonry building when the displacement of the roof equals 49.963 mm, point A in Fig. 17

5 CONCLUSION

The paper presents nonlinear analysis of unreinforced masonry buildings. The analysis is used finite element procedure and a close form solution proposed by Akhaveissy [1]. The close form solution was determined based on a new interface model for modeling the mechanical response of mortar joints in masonry walls. The interface laws were formulated in the framework of elasto-plasticity for non-standard materials with softening, which occurs in mortar joints because of applied shear and tensile stresses. The Von Mises criterion was used to simulate the behavior of the units. The interface laws for contact elements were formulated to simulate the softening behavior of mortar joints under tensile stress. A normal linear cap model was also used to limit compressive stress. The capabilities of the interface model and the effectiveness of the computational procedure were investigated using numerical examples that simulate the response of a masonry wall tested under shear in the presence of an initial pre-compression load. The computer predictions correlated very well with the test data. The closed-form solution was better than ATC and FEMA 273 at predicting the ultimate lateral load of unreinforced masonry walls. Hence in the present work, the new closed-form solution is implemented in a finite element method using two-noded linear elements. An algorithm is presented for this purpose. Different masonry structures, including low- and high-rise masonry buildings, are analyzed using the new closed-form solution and the presented algorithm. A comparison of results from the present work with experimental data and previous works show proper accuracy from the present work. Consequently, the proposed closed-form solution and the presented algorithm can be used to satisfactorily analyze masonry structures similar to those considered in this work. The finite element method with two-noded linear element and presented algorithm show proper accuracy for analysis of low- and high-rise unreinforced masonry buildings. Hence, the proposed model can be used to predict the base shear force of unreinforced masonry structures under earthquake acceleration in nonlinear finite element analyses. Therefore, practicing engineers can determine the behavior of an URM building and its performance level with proper accuracy under seismic excitation using concepts described in the present work.

References

[1] A.H. Akhaveissy. Lateral strength force of URM structures based on a constitutive model for interface element. *Latin American Journal of Solids and Structures*, 8:445–461, 2011.

[2] A.H. Akhaveissy and C.S. Desai. Unreinforced masonry walls: Nonlinear finite element analysis with a unified constitutive model. *Archives of Computational Methods in Engineering*, 18:485–502, 2011.

[3] C. Alessandri and C.A. Brebbia. Strength of masonry walls under static horizontal loads: boundary element analysis and experimental tests. *Engineering Analysis*, 4(3):118–134, 1987.

[4] Y. Belmouden and P. Lestuzzi. An equivalent frame model for seismic analysis of masonry and reinforced concrete buildings. *Construction and Building Materials*, 23:40–53, 2009.

[5] A. Brencich, L. Gambarotta, and S. Lagomarsino. A macroelement approach to the three-domensional seismic analysis of masonry buildings. In *11th European Conference on Earthquake Engineering*, Rotterdam, 1998. Balkema. ISBN 9054109823.

[6] A. Brencich, L. Gambarotta, and S. Lagomarsino. Analysis of a masonry building in via martoglio. pages 107–143, 2000. Catania Project: Research on the seismic response of two masonry buildings, chapter 6, University of Genoa (in Italian), CNR Gruppo Nazionale per la Difesa dei Terremoti.

[7] M. Bruneau. State-of-the-art report on seismic performance of unreinforced masonry buildings. *Journal of Structural Engineering*, 120(1):230–251, 1994.

[8] C. Calderini, S. Cattari, and S. Lagomarsino. In plane seismic response of unreinforced masonry walls: comparison between detailed and equivalent frame models. In M. Papadrakakis, N.D. Lagaros, and M. Fragiadakis, editors, *COMPDYN 2009, ECCOMAS Thematic Conference on Computational Methods in Structural Dynamics and Earthquake Engineering In*, pages 22–24, Rhodes, Grecce, June 2009.

[9] A. Cecchi and G. Milani. A kinematic fe limit analysis model fot thick english bond masonry walls. *International Journal of Solids and Structures*, 45:1302–1331, 2008.

[10] K. Chaimoon and M.M. Attard. Experimenatl and numerical investigation of masonry under three-point bending (in-plane). *Engineering Structures*, 31:103–112, 2009.

[11] I.O. Demirel. *A nonlinear equivalent frame model for displacement based analysis of unreinforced brick masonry buildings*. Dissertation, Middle East Technical University, 2010.

[12] Federal Emergency Management Agency (FEMA-307), Washington (DC). *Evaluation of earthquake damaged concrete and masonry wall buildings*, 1999. Technical Resources Publication no. 307.

[13] Federal Emergency Management Agency (FEMA-356), Washington (DC). *NEHRP Guidelines for the seismic rehabilitation of buildings*, 2000.

[14] A. Gabor, E. Ferrier, Jacquelin, and P. Hamelin. Analysis and modeling of the in-plane shear behavior of hollow brick masonry panels. *Construction and Building Materials*, 20:308–321, 2006.

[15] H.B. Kaushik, D.C. Rai, and S.K. Jain. Stress-strain characteristics of clay brick masonry under uniaxial compression. *Journal of Material in Civil Engineering ASCE*, 19(9):728–739, 2007.

[16] H.B. Kaushik, D.C. Rai, and S.K. Jain. Uniaxial compressive stress-strain model for clay brick masonry. *Current Science*, 92(4):497–501, 2007.

[17] J. Lopez, S. Oller, E. Onate, and J. Lubliner. A homogeneous constitutive model for masonry. *Int. J. Numer. Meth. Engng.*, 46:1651–1671, 1999.

[18] G. Magenes and G.M. Calvi. In-plane seismic response of brick masonry walls. *Earthquake Engineering and Structural Dynamics*, 26:1091–1112, 1997.

[19] C.S. Meisl, K.J. Elwood, and C.E. Ventura. Shake table tests on the out-of-plane response of unreinforced masonry walls. *Canadian Journal Civil Engineering*, 34:1381–1392, 2007.

[20] G. Milani. Simple homogenization model for the non-linear analysis of in-plane loaded masonry walls. *Computers and Structures*, 89:1586–1601, 2011.

[21] G. Milani. Simple lower bound limit analysis homogenization model for in-and out-of-plane loaded masonry walls. *Construction and Building Materials*, 25:4426–4443, 2011.

[22] G. Milani, K. Beyer, and A. Dazio. Upper bound limit analysis of meso-mechanical spandrel models for the pushover analysis of 2D masonry frames. *Engineering Structures*, 31:2696–2710, 2009.

[23] G. Milani, P. Lourenco, and A. Tralli. Homogenised limit analysis of masonry walls, part i: Failure surfaces. *Computers and Structures*, 84:166–180, 2006.

[24] G. Milani, P. Lourenco, and A. Tralli. 3D homogenized limit analysis of masonry buildings under horizontal loads. *Engineering Structures*, 29:3134–3148, 2007.

[25] G. Milani, P.B. Lourenco, and A. Tralli. Homogenised limit analysis of masonry walls, part ii: Structural examples. *Computers and Structures*, 84:181–195, 2006.

[26] G. Milani, E. Miani, and A. Tralli. Approximate limit analysis of full scale FRP-reinforced masonry buildings through a 3D homogenized fe package. *Composite Structures*, 92:918–935, 2010.

[27] J. Paquette and M. Bruneau. Pseudo- dynamic testing of unreinforced masonry building with flexible diaphragm. *Journal of Structural Engineering ASCE*, 129(6):708–716, 2003.

[28] J. Paquette and M. Bruneau. Pseudo- dynamic testing of unreinforced masonry building with flexible diaphragm. In *In: 13th World Conference on Earthquake Engineering Vancouver*, B.C., Canada, paper 2609, 2004.

[29] J. Paquette and M. Bruneau. Pseudo- dynamic testing of unreinforced masonry building with flexible diaphragm and comparison with existing procedures. *Construction and Building Materials*, 20:220–228, 2006.

[30] J. Park, P. Towashiraporn, J.I. Craig, and B.J. Goodno. Seismic fragility analysis of low-rise unreinforced masonry structures. *Engineering Structures*, 31:125–137, 2009.

[31] L. Pasticier, C. Amadio, and M. Fragiacomo. Non-linear seismic analysis and vulnerability evaluation of a masonry building by means of the sap2000 v.10 code. *Earthquake Engineering and Structural Dynamics*, 37:467–485, 2008.

[32] P. Roca. Assessment of masonry shear-walls by simple equilibrium models. *Construction and Building Materials*, 20:229–238, 2006.

[33] M. Rota, A. Penna, and G. Magenes. A methodology for deriving analytical fragility curves for masonry buildings based on stochastic nonlinear analyses. *Engineering Structures*, 32:1312–1323, 2010.

[34] T. Salonikios, C. Karakostas, V. Lekidis, and A. Anthoine. Comparative inelastic pushover analysis pf masonry frames. *Engineering Structures*, 25:1515–1523, 2003.

[35] I. Sharif, C.S. Meisl, and K.J. Elwood. Assessment of asce 41 height-to-thickness ratio limits for urm walls. *Earthquake Spectra*, 23(4):893–908, 2007.

[36] M. Shariq, H. Abbas, H. Irtaza, and M. Qamaruddin. Influence of openings on seismic performance of masonry building walls. *Building and Environment*, 43:1232–1240, 2008.

[37] A. Tena-Colunga, A. Juarez-Angeles, and V.H. Salinas-Vallejo. Cyclic behavior of combined and confined masonry walls. *Engineering Structures*, 31:240–259, 2009.

[38] G. Vasconcelos and P.B. Lourenco. Experimental characterization of stone masonry in shear and compression. *Construction and Building Materials*, 23:3337–3345, 2009.